

Ginzburg-Landau Theory for Impure Superfluid ^3He

E.V. Thuneberg

Low Temperature Laboratory, Helsinki University of Technology, P.O. Box 2200,
02015 TKK, Finland

Abstract. Liquid ^3He at low temperatures is an ideal substance to study because of its natural purity. The superfluid state, which appears at temperatures below 3 mK, has many unusual and exciting properties. These have extensively been studied experimentally, and the results are in many cases well understood theoretically using quasiclassical approximation. In this work we study the case that liquid ^3He is inside of aerogel. Aerogel is a very porous substance, where 98% of the volume can be empty. The purpose is to understand how the properties of the superfluid are modified when the quasiparticles are scattered from an impurity, such as aerogel. We study extensively the *homogeneous scattering model*. From it we derive the Ginzburg-Landau theory of impure superfluid ^3He . We give expressions for measurable quantities and compare them with experiments. We consider random anisotropy and its effect on the NMR properties. More sophisticated scattering models are briefly discussed.¹

1 Introduction

Liquid ^3He at low temperatures is the purest substance in Nature because usual impurities simply will fall down by gravity. This is one of the reasons why liquid ^3He , in spite of its strong particle-particle interactions, is one of the best understood condensed matter systems (Vollhardt and Wölfle 1990). Especially the superfluid state, which occurs at temperatures below 3 mK, shows many complicated but still well understood phenomena. But the purity can also be a limitation because often important physical effects exist only because of impurities. For example, except of a few marginal cases, all pure elemental superconductors are of type I. That is, type II superconductivity, where magnetic field penetrates into the superconductor as quantized flux lines, exist because of impurities which radically change the properties of pure elements.

One type of impurity is formed by the surfaces of the container that hold the liquid. There has been several studies of liquid ^3He in different confined geometries, for example between parallel plates or in packed powders (for example, Tholen and Parpia 1992). In these cases the effect on ^3He arises from walls, i.e. from 2-dimensional interfaces between ^3He and a foreign object. It is very difficult to support zero-dimensional (point-like) impurities in liquid ^3He . However, there is the intermediate case of one-dimensional impurities. This type of

¹ Work done in collaboration with M. Fogelström, S.K. Yip, J.A. Sauls, R. Hänninen, and T. Setälä

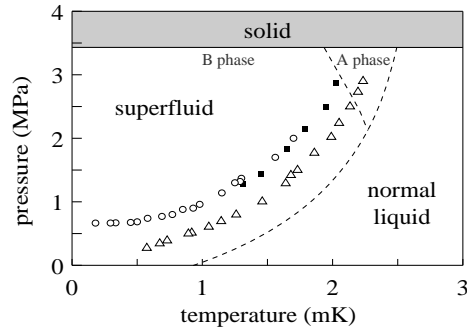


Fig. 1. The measured superfluid transition points of ^3He in aerogel: Porto and Parpia (1995, \triangle), Sprague et al. (1995, \blacksquare), and Matsumoto et al. (1997, \circ). The dashed lines denote the normal-superfluid and the A-B transition lines in pure ^3He . The A and B phases also refer to pure ^3He .

impurity can approximately be realized by silica aerogels. These are very porous materials where, for example, 98% of the volume is empty. Several recent experiments investigate ^3He in aerogel (Porto and Parpia 1995, Matsumoto et al. 1997, Sprague et al. 1995, 1996). It is found that, similar to the bulk liquid, ^3He in aerogel goes to the superfluid state, but both the superfluid transition temperature T_c and the amplitude of the superfluid state are reduced compared to the pure case. The measured suppression of T_c is shown in Fig. 1.

In this article we present some theoretical ideas concerning ^3He in aerogel. We first describe the structure of aerogel (Section 2). The main effect of aerogel on superfluid ^3He arises from scattering of the quasiparticles of ^3He from the aerogel impurity. This effect can be calculated to a good approximation using the quasiclassical theory. The general assumptions of quasiclassical scattering models are discussed in Section 3. In Section 4 we study a model where the scattering is considered as homogeneously distributed. We will limit to temperatures in the neighborhood of the transition temperature T_c , and derive the Ginzburg-Landau theory. We calculate measurable quantities and compare them with experiments. We find that more sophisticated scattering models are needed in order to explain the measurements quantitatively (Section 5). The anisotropy of the scattering is considered in Section 6. There we study a random field model using similar arguments as presented by Imry and Ma (1975), and find that the NMR properties crucially depend on the anisotropy.

2 Aerogel

A nice introduction to aerogels is given by Fricke (1988). The fabrication uses a gelation process in the liquid phase. A variety of *aerogel* materials are possible, but the present ones are of silica, $(\text{SiO}_2)_n$. In order to get *aerogel* it is crucial to preserve the gel structure when the solvent is removed. This is not trivial because the surface tension of the liquid–gas interface would make the gel to collapse in straightforward drying. Fortunately, it is possible to go continuously from the liquid to the gas phase. For that one has to move along such a path that goes around the critical point (T_0, p_0) in the temperature–pressure plane. In order to avoid too high temperatures and pressures, methanol (512 K, 8 MPa) is preferred to water (647 K, 22 MPa) as a solvent.

The experiments with superfluid ^3He use samples where the aerogel fills only 2% of the total volume, $V = 0.02$. The surface to volume ratio is determined by measurements with ^4He , and they give $A = 260000 \text{ cm}^{-1}$ (Kim et al. 1993). Based on these numbers alone, we can make some estimations of the dimensions in aerogel. If we assume that the structure is a lattice of one-dimensional strands, we calculate the strand diameter $4V/A = 3 \text{ nm}$ and the distance between neighboring strands $\sqrt{4\pi V}/A = 20 \text{ nm}$. The mean free path for straight line trajectories is estimated as $\ell = 4/A = 150 \text{ nm}$. Although this picture is certainly very idealized, the numbers are not very different from the ones obtained by other means such as transmission electron microscopy or low-angle x-ray scattering. The distance between strands certainly has large variation because of fluctuations in the local aerogel density.

The next step in understanding superfluid ^3He in aerogel is to study the characteristic lengths of ^3He . The smallest scale is the average distance between neighboring ^3He atoms. This is on the same order of magnitude as the Fermi wave length $\lambda_f = 2\pi/k_f \approx 0.7 \text{ nm}$. This is somewhat smaller than the diameter of the strands. A much larger scale is the coherence length $\xi_0 = \hbar v_f/2\pi k_B T_{c0}$. Here T_{c0} is the superfluid transition temperature in bulk ^3He and v_f is the Fermi velocity. As a function of pressure, ξ_0 decreases monotonically from 77 nm (zero pressure) to 16 nm (3.4 MPa, the solidification pressure). The coherence length is on the same order as the average strand spacing, but taking into account fluctuations in strand density, we can well expect voids of size larger than ξ_0 . Finally, the mean free path of quasiparticles in pure ^3He is 1 μm or more at the temperatures we are interested in ($T < 3 \text{ mK}$). Thus the scattering from strands is the dominant factor that limits the mean free path in aerogel.

3 Quasiclassical Scattering Models

Before going into the details of different scattering models, it is useful to study the general assumptions. Large part of the ideas presented here are given in a more mathematical form by Buchholtz and Rainer (1979). The following is applicable to both metals and ^3He at low temperatures. Here a “particle” refers

to an electron in the former case and to a ^3He atom in the latter. “Superfluidity” denotes both the superconductivity of metals and the superfluidity of ^3He . The many-body hamiltonian of the system can be written as

$$H = H_{\text{pure}} + \sum_j V_j . \quad (1)$$

Here H_{pure} contains the kinetic energies of the particles and interactions between them, and also interaction with the periodic crystal lattice in the case of metals. It may also contain the interaction with external magnetic field, for example. The latter term is the impurity potential. In the case of metals, a common source for it is that some atoms of the lattice are of different type than the others. In the case of ^3He , such a term is introduced by the aerogel. Quite generally, the total impurity potential V can be written as a sum so that each term V_j is nonzero only in some small region of space. These regions are referred to as “scattering centers”.

The general quasiclassical theory for H_{pure} is discussed extensively by Serene and Rainer (1983), and also elsewhere in this book. The validity of this theory for the superfluid state relies on the assumption $\lambda_f \ll \xi_0$, which is well satisfied in ^3He and in most superconductors. The result is that instead of strongly interacting particles, the system is better understood in terms of quasiparticles. The quasiparticles propagate through the medium similar to classical particles. The interactions between the quasiparticles are weak, and can be neglected in many cases, which would not be the case for particles. Such quasiclassical description is valid for properties that are dominated by processes taking place near the Fermi surface in the momentum space. This includes virtually all phenomena in the superfluid state.

Let us consider adding the impurity effects to the quasiclassical theory. We will not set a limitation to the magnitude of the impurity potential i.e. it can be large, on the order of the Fermi energy E_f . The crucial assumption is that this large potential occurs only in a limited volume of the total space. This means that the quasiparticle description is still valid in most of the space. The average distance a quasiparticle can travel between it collides with scattering centers defines a mean free path ℓ . In order to use the quasiparticle picture, ℓ has to be large in comparison to the Fermi wave length λ_f . In addition, we neglect coherent scattering from two or more scattering centers. This is justified to leading order in λ_f/ℓ as long as the locations of the scattering centers can be considered random on the scale of λ_f . In other words, the interference can be neglected in an ensemble average if for each scattering center j we have a distribution function $n_j(\mathbf{r})$ ($\int d^3r n_j(\mathbf{r}) = 1$) that is smooth on the scale of λ_f . Note that $n_j(\mathbf{r})$ can still be a good approximation to the delta function when looked at on the scale of ξ_0 . In the case that all scattering centers are identical, it is sufficient to specify only one distribution $n(\mathbf{r})$, which is normalized to the total number N of scattering centers: $\int d^3r n(\mathbf{r}) = N$

In a small neighborhood of a scattering center, the state of the system can be strongly different from the bulk. For example, liquid ^3He may be in a solid-like

state because of the van der Waals interaction with an impurity. In order to allow such changes, the treatment within a scattering center must be fully quantum mechanical. However, such a calculation is not possible in practice because even the wave function of a quasiparticle is not known in any detail. Therefore, one has to introduce the properties of a scattering center by some phenomenological parameters. A sufficient description is to know the scattering T matrix or, in case of an isotropic scattering center, the scattering phase shifts δ_l . It is important to notice that these are parameters that appear in the normal state, and they can in principle be measured without need to go into the superfluid state.

The discussion above was limited to the neighborhood of the Fermi surface, where the quasiparticle picture is valid. Because of their strong potential, the impurities also have an effect outside of this range. As a consequence the pairing interaction, for example, is modified by the impurities. However, this effect is of short range because of the relatively high energy. Therefore we can neglect such effects relying on the assumption that the volume fraction of the scattering centers is small. Similar argument gives that the Landau Fermi-liquid parameters (F_i^s, F_i^s), as well as the density (ρ) and the dipole-dipole interaction constant (g_d) in ^3He are unchanged.

The size of a scattering center has to be small compared to the length scale one is interested to study. In the superfluid state this scale is typically set by the coherence length ξ_0 . Thus a scattering center has to be small compared to ξ_0 , although it can be large compared to λ_f . It should be noted that the size of the scattering center does not limit the size of the impurity. In order to consider a macroscopic body, we represent its surface by a set of scattering centers. This is possible because for all practical bodies, the height-height correlations $\langle \zeta(\mathbf{r})\zeta(\mathbf{r} + \delta\mathbf{r}) \rangle$ of the surface have a distribution that is much wider than λ_f when the separation δr is on the order of ξ_0 . Thus the scattering becomes incoherent on this scale, and therefore can be represented by different scattering centers. Assuming that the particles cannot penetrate into the body, the volume of the body should be excluded from the calculation. For example, we estimate the volume of scattering centers in aerogel as the volume of few atomic layers on the strands ($\approx \lambda_f A$) rather than the volume of the strands themselves (V). (It happens, however, that both quantities are on the same order of magnitude in this case).

Let us comment the effect of the pairing state. Superfluidity arises because part of the quasiparticles are weakly bound to pairs. The momenta of the quasiparticles in a pair can be denoted by \mathbf{p} and $-\mathbf{p}$ because the total momentum of the pair is small. The dependence of the pair wave function on the direction $\hat{\mathbf{p}} = \mathbf{p}/p$ can be described using spherical harmonic functions and classified as s, p, d , etc. states. In most superconducting metals the Cooper pairs form dominantly in an s -wave state. In ^3He the pairs form in a p -wave state, and there is increasing evidence that d waves are dominant in high- T_c cuprate superconductors. The amplitude of the superfluid state and the transition temperature can be calculated for these cases as a function of impurity scattering, as will be discussed in more detail later. In the quasiclassical approximation one finds that the

impurities have no effect on a homogeneous s -wave superfluid. For other waves the superfluidity is suppressed by impurity, and it disappears when the mean free path is reduced to $\sim \xi_0$. The interpretation is that scattering changes the momenta of the quasiparticles, but this has no effect in the s -wave case because the wave function is independent of the momentum direction. For other waves the sign of the wave function changes for certain scattering angles, which leads to destructive interference. There is an effect for s waves, too, if the superfluid state is inhomogeneous. Here the scattering makes the quasiparticles more localized, and therefore they see more the same order parameter. This effect makes the superconductor less sensitive to magnetic field, i.e. causes the change from type I to type II superconductivity, as mentioned in the introduction.

All the discussion above has been in weak-coupling limit. This means neglecting all corrections that are proportional to the small ratio λ_f/ξ_0 . This approximation is clearly inadequate for some properties of ^3He . For example, it gives that the B phase is always more stable than the A phase, contrary to the phase diagram in Fig. 1. There are some calculations of strong coupling corrections in the pure ^3He (Serene and Rainer 1983). It seems very difficult to take these corrections into account in the impure case, and therefore we do not consider them here.

4 Homogeneous Scattering Model

We do not know the precise distribution $n(\mathbf{r})$ of scattering centers in aerogel. Therefore we have to take a model for $n(\mathbf{r})$. The simplest possible one is the homogeneous scattering model (HSM). There one assumes that $n(\mathbf{r}) = n$ is a constant. In other words, the probability for a quasiparticle to be scattered is the same at all locations \mathbf{r} . This same approximation is commonly used to study impurities in superconductors (Gorkov 1959, Abrikosov and Gorkov 1961).

The mean free path in the HSM is given by $\ell = (n\sigma)^{-1}$. Here σ is the scattering cross section of a scattering center. We additionally assume that the medium is isotropic, i.e. ℓ is independent of the direction of quasiparticle momentum. We also assume that the scattering is nonmagnetic. This means that the scattering probability is the same for both directions of the spin, and the spin is not changed in the scattering.

A convenient property of the isotropic HSM is that both the Ginzburg-Landau (GL) theory and Leggett's theory of NMR (Leggett 1974) have the same form as in pure ^3He . The changes appear only via modified parameter values of these theories. The GL theory allows a convenient way to represent the results of the HSM at temperatures near T_c . Therefore we describe it in detail below.

The order parameter in superfluid ^3He is a complex 3×3 matrix $A_{\mu i}$. This describes the wave function of the Cooper pairs such that for a given direction $\hat{\mathbf{p}}$ of momentum, the (unnormalized) spin wave function is given by (Leggett 1975)

$$\psi_{\text{spin}}(\hat{\mathbf{p}}) = (-d_x + id_y)|\uparrow\uparrow\rangle + d_z|\uparrow\downarrow + \downarrow\uparrow\rangle + (d_x + id_y)|\downarrow\downarrow\rangle, \quad (2)$$

where $d_\mu = \sum_i A_{\mu i} \hat{p}_i$. This apparently strange notation has the advantage that the spin μ and the orbital i indices in $A_{\mu i}$ transform equally in coordinate rotations. The amplitude of $A_{\mu i}$ describes how strong the superfluid state is. In particular, it goes to zero continuously when the temperature approaches the superfluid transition temperature T_c .

The free energy f of the superfluid is a function of the order parameter $A_{\mu i}$. Similar to the Ginzburg-Landau theory of superconductivity, one can expand f in powers of $A_{\mu i}$ when the temperature is not much different from T_c . The most important ‘‘bulk’’ terms in the expansion are (Mermin and Stare 1973)

$$f_{\text{bulk}} = f_n + \alpha A_{\mu i}^* A_{\mu i} + \beta_1 |A_{\mu i} A_{\mu i}|^2 + \beta_2 (A_{\mu i} A_{\mu i}^*)^2 + \beta_3 A_{\mu i}^* A_{\nu i}^* A_{\nu j} A_{\mu j} + \beta_4 A_{\mu i}^* A_{\nu i} A_{\nu j}^* A_{\mu j} + \beta_5 A_{\mu i}^* A_{\nu i} A_{\nu j} A_{\mu j}^* . \quad (3)$$

Here a summation over repeated indices is implied. Equation (3) includes the allowed terms up to fourth order, since several terms have to vanish by symmetry: f has to be real valued, and it should remain unchanged in rotations of both the spin and the orbital parts of $A_{\mu i}$. This is because the pairing interaction is unchanged in such rotations. For stability the fourth order terms have to be positive definite, but otherwise the coefficients β_i are arbitrary in a phenomenological approach.

Minimizing (3) one finds the normal state ($A_{\mu i} = 0$) when $\alpha > 0$. In the superfluid state ($\alpha < 0$) there are several possible minima. The most important are the ones corresponding to the A and B phases. The order parameter in the B phase has the form

$$A_{\mu j} = \exp(i\vartheta) \Delta_B R_{\mu j} , \quad (4)$$

where $R_{\mu i}$ is an arbitrary rotation matrix ($R_{\mu i} R_{\mu j} = \delta_{ij}$), ϑ an arbitrary phase, and

$$f_B - f_n = \frac{3}{2} \alpha \Delta_B^2 = -\frac{3\alpha^2}{4(3\beta_{12} + \beta_{345})} . \quad (5)$$

We use the notation $\beta_{ij\dots} = \beta_i + \beta_j + \dots$. The A phase has

$$A_{\mu j} = \Delta_A \hat{d}_\mu (\hat{m}_j + i\hat{n}_j) , \quad (6)$$

where $\hat{\mathbf{d}}$ is an arbitrary unit vector and $\hat{\mathbf{m}}$, $\hat{\mathbf{n}}$, and $\hat{\mathbf{l}} = \hat{\mathbf{m}} \times \hat{\mathbf{n}}$ from an arbitrary orthonormal triad. The energy and amplitude are

$$f_A - f_n = \alpha \Delta_A^2 = -\frac{\alpha^2}{4\beta_{245}} . \quad (7)$$

In order to get the coefficients α and β_i one has to solve the quasiclassical equations. This is briefly explained in the Appendix. The result for α is

$$\alpha = \frac{N(0)}{3} \left[\ln \frac{T}{T_{c0}} + \sum_{n=1}^{\infty} \left(\frac{1}{n - \frac{1}{2}} - \frac{1}{n - \frac{1}{2} + x} \right) \right] , \quad (8)$$

where $2N(0)$ is the density of states at the Fermi surface and $x = \hbar v_f / 4\pi T \ell_{\text{tr}}$. The scattering parameter is the *transport* mean free path $\ell_{\text{tr}} = (n\sigma_{\text{tr}})^{-1}$. The

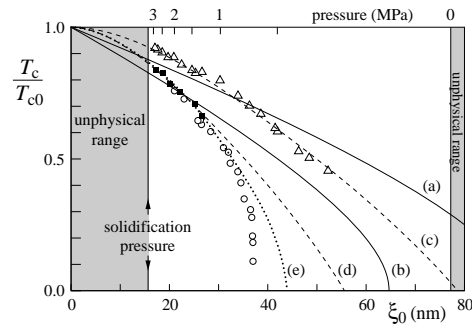


Fig. 2. The transition temperature in aerogel relative to that in bulk, T_c/T_{c0} . The horizontal axis is the coherence length $\xi_0 = \hbar v_f / 2\pi k_B T_{c0}$. The experimentally inaccessible values of ξ_0 are denoted by shading. The data points are the same as in Fig. 1: Porto and Parpia (1995, \triangle), Sprague et al. (1995, \blacksquare), and Matsumoto et al. (1997, \circ). The solid lines correspond to the homogeneous scattering model (HSM) at mean free paths $\ell_{\text{tr}} = 320$ nm (a) and 230 nm (b), and the dashed lines correspond to slabs of thicknesses $D = 105$ nm (c) and 74 nm (d). The dotted line is the isotropic inhomogeneous scattering model (IISM) with average mean free path 70 nm, unit cell radius $R = 140$ nm, and scattering profile parameter $j = 8$.

transport cross section σ_{tr} gives more weight to large scattering angles θ than the total cross section σ . The precise definitions are $\sigma_{\text{tr}} = 4\pi \langle (1 - \cos \theta) (d\sigma/d\Omega)(\theta) \rangle_{\Omega}$ and $\sigma = 4\pi \langle (d\sigma/d\Omega)(\theta) \rangle_{\Omega}$. Here $(d\sigma/d\Omega)(\theta)$ is the differential scattering cross section and $\langle \dots \rangle_{\Omega}$ denotes average over 4π solid angle.

The α term (8) was first calculated by Larkin (1965). It has exactly the same form as calculated earlier for *magnetic* impurities in *s*-wave superfluid (Abrikosov and Gorkov 1961). The transition temperature T_c obtained from the condition $\alpha(T_c) = 0$ is plotted in Fig. 2. The figure also shows the experimental data plotted as a function of the coherence length ξ_0 . We see that the HSM gives a suppression of T_c , but its dependence on ξ_0 is much weaker than is seen experimentally.

We have assumed in Fig. 2 that ℓ_{tr} is a pressure-independent constant. We can identify three effects that could make $\ell_{\text{tr}} = (n\sigma_{\text{tr}})^{-1}$ pressure dependent. (i) The structure of aerogel changes. (ii) The Fermi momentum changes. (iii) The wave function of a quasiparticle changes. It seems that all these effects are negligible compared to the changes shown in Fig. 2. In particular, the Fermi momentum $\hbar k_f$ changes only 10% over the whole pressure range, and calculations with hard spheres indicate that σ_{tr} is very weakly dependent on k_f for impurities that are large compared to λ_f . What remains most uncertain is point (ii) because we do not know the wave function of a quasiparticle and how it changes with pressure.

In the neighborhood of the transition temperature T_c we expand $\alpha(T) =$

$\alpha' \times (T/T_c - 1)$. The higher order corrections in the Taylor series are dropped because they would not improve the accuracy of the GL functional (3). From equation (8) one easily gets

$$\alpha' = \frac{N(0)}{3} \left[1 - x_c \sum_{n=1}^{\infty} (n - \frac{1}{2} + x_c)^{-2} \right], \quad (9)$$

where $x_c = \hbar v_f / 4\pi T_c \ell_{\text{tr}}$.

It is not easy to calculate the fourth order coefficients β_i with the same generality as α . Therefore we make the additional assumption that only the s -wave scattering phase shift δ_0 is nonzero. In this case $\sigma_{\text{tr}} = \sigma$, and we get

$$\begin{pmatrix} \beta_1 \\ \beta_2 \\ \beta_3 \\ \beta_4 \\ \beta_5 \end{pmatrix} = a \begin{pmatrix} -1/2 \\ 1 \\ 1 \\ 1 \\ -1 \end{pmatrix} + b \begin{pmatrix} 0 \\ 1 \\ 0 \\ 1 \\ -1 \end{pmatrix} + \begin{pmatrix} \Delta\beta_1^{\text{sc}} \\ \Delta\beta_2^{\text{sc}} \\ \Delta\beta_3^{\text{sc}} \\ \Delta\beta_4^{\text{sc}} \\ \Delta\beta_5^{\text{sc}} \end{pmatrix} \quad (10)$$

$$a = \frac{N(0)}{120(\pi T_c)^2} \sum_{n=1}^{\infty} (n - \frac{1}{2} + x_c)^{-3}$$

$$b = \frac{N(0)\hbar v_f}{288(\pi T_c)^3 \ell} (\sin^2 \delta_0 - \frac{1}{2}) \sum_{n=1}^{\infty} (n - \frac{1}{2} + x_c)^{-4}.$$

Here $\Delta\beta_j^{\text{sc}}$ are strong-coupling corrections which are not evaluated here. A model calculation for them in pure ^3He is given by Sauls and Serene (1980).

Note that α and a , instead of depending separately on n and the cross section $\sigma = (4\pi/k_f^2) \sin^2 \delta_0$, depend only on the combination $\ell = (\sigma n)^{-1}$. This is not the case for b , which is also a function of δ_0 . The limiting cases $\sin^2 \delta_0 \rightarrow 0$ and $\sin^2 \delta_0 = 1$ are known as Born and unitarity limits, respectively. This additional degree of freedom decreases the precision of the theoretical results because δ_0 is not generally known. However, we argue in the following that this degree of freedom is averaged out in aerogel. Firstly, if the impurities are not identical, we can expect that there is a distribution of δ_0 's instead of a single value. Secondly, the calculation including all partial waves has been done in the case of B phase (Thuneberg et al. 1981). There one finds a similar spread of the results as a function of the phase shifts. But for large impurities the phase shifts δ_l with different l are essentially random, as demonstrated by δ_l for hard spheres. Both these arguments support that a reasonable guess, if no more detailed information exists, is to assume random phase shifts $\sin^2 \delta_0 \rightarrow 0.5$.

A necessary condition for the stability of the A phase is $f_A < f_B$. Using equations (5), (7), and (10) this reduces to

$$a < 6\Delta\beta_1^{\text{sc}} + 2\Delta\beta_3^{\text{sc}} - 4\Delta\beta_4^{\text{sc}}. \quad (11)$$

Because a increases monotonically by factor 3 with decreasing T_c , the B phase becomes more favored with increasing scattering assuming that $\Delta\beta_j^{\text{sc}}$ do not

grow even more. Assuming $\Delta\beta_j^{\text{sc}}$ remain constants, we can expect stable A phase only at temperatures (in mK) and pressures where it is stable in the pure case. Calculations with other phases indicate that they are not serious competitors to A and B phases.

In order to make more comparisons with experiments, we need to consider additional terms in the GL functional $F = \int d^3r f(\mathbf{r})$. These are the gradient energy

$$f_{\text{k}} = K [(\gamma - 1)\partial_i A_{\mu i} \partial_j A_{\mu j}^* + \partial_i A_{\mu j} \partial_i A_{\mu j}^*] , \quad (12)$$

the energy of the magnetic field \mathbf{H} ,

$$f_{\text{z}} = -\frac{1}{2}\chi_{\text{n}}^{-1}H^2 + g_{\text{z}}H_{\mu}A_{\mu i}A_{\nu i}^*H_{\nu} , \quad (13)$$

where χ_{n} is the susceptibility of the normal state, and the magnetic dipole-dipole interaction energy

$$f_{\text{d}} = g_{\text{d}}(|A_{ii}|^2 + A_{ij}A_{ji}^* - \frac{2}{3}A_{\mu i}A_{\mu i}^*) . \quad (14)$$

Here f_{k} is purely phenomenological similar to the bulk energy (3), but in f_{z} and f_{d} we have dropped some terms, which could be there in a pure phenomenological theory. For the coefficients we calculate (Appendix)

$$K = \frac{N(0)\hbar^2 v_{\text{f}}^2}{240\pi^2 T_{\text{c}}^2} \sum_{n=1}^{\infty} (n - \frac{1}{2} + x_{\text{c}})^{-3} \quad (15)$$

$$\gamma = 3 + \frac{5\hbar v_{\text{f}}}{12\pi T_{\text{c}} \ell} \frac{\sum_{n=1}^{\infty} (n - \frac{1}{2})^{-1} (n - \frac{1}{2} + x_{\text{c}})^{-3}}{\sum_{n=1}^{\infty} (n - \frac{1}{2} + x_{\text{c}})^{-3}} \quad (16)$$

$$g_{\text{z}} = \frac{\hbar^2 \tilde{\gamma}^2 N(0)}{48\pi^2 T_{\text{c}}^2 (1 + F_0^{\text{a}})^2} \sum_{n=1}^{\infty} (n - \frac{1}{2} + x_{\text{c}})^{-3} \quad (17)$$

$$g_{\text{d}} = \frac{\mu_0}{40} \left[\hbar \tilde{\gamma} N(0) R \sum_{n=1}^{\epsilon_{\text{cut off}}/2\pi T_{\text{c}}} (n - \frac{1}{2} + x_{\text{c}})^{-1} \right]^2 , \quad (18)$$

where $\tilde{\gamma}$ is the gyromagnetic ratio, F_0^{a} a Fermi-liquid parameter, R a renormalization constant for the dipole energy, and $\epsilon_{\text{cut off}}$ a high-energy cut-off (Leggett 1974). The dipole-dipole coupling constant g_{d} is different from the other coefficients [(8)-(10), (15)-(17)] because it is dominated by high-energy processes (it would diverge for $\epsilon_{\text{cut off}} \rightarrow \infty$), and therefore it is a constant (independent of scattering).

All the coefficients above reduce to the well know GL coefficients in the limit vanishing scattering, $\ell \rightarrow \infty$ (Fetter 1975, Thuneberg 1987).

In most cases the terms f_{z} and f_{d} are small compared to f_{bulk} . Treating them as perturbations, we find in the A phase (apart from constants)

$$f_{\text{zA}} = -\frac{1}{2}\chi_{\text{n}}^{-1}H^2 + g_{\text{z}}\Delta_{\text{A}}^2(\hat{\mathbf{d}} \cdot \mathbf{H})^2 \quad (19)$$

$$f_{\text{dA}} = -2g_{\text{d}}\Delta_{\text{A}}^2(\hat{\mathbf{d}} \cdot \hat{\mathbf{i}})^2 , \quad (20)$$

which favor $\hat{\mathbf{d}} \perp \mathbf{H}$ and $\hat{\mathbf{d}} \parallel \hat{\mathbf{I}}$, respectively. The B phase is slightly more complicated. We parameterize the rotation matrix $R_{\mu i}$ by an angle θ and an axis $\hat{\mathbf{n}}$ of rotation. The dipole-dipole energy f_d favors $\theta = \arccos(-1/4) = 104^\circ$. The external field leads to distortion of B phase order parameter (4). This gives rise to the energy term

$$f_{dzB} = -\frac{5g_d g_d}{4\beta_{345}} (\hat{\mathbf{n}} \cdot \mathbf{H})^2, \quad (21)$$

which favors $\hat{\mathbf{n}} \parallel \mathbf{H}$.

For comparison to experiments, we still need to relate the observables to the GL coefficients. The torsional oscillator experiments measure the superfluid density ρ_s (Porto and Parpia 1995, Matsumoto et al. 1997). This can be calculated by evaluating f_k (12) in the presence of a phase gradient: $\nabla A_{\mu j} = i\mathbf{q}A_{\mu j}$, where the superfluid velocity $\mathbf{v}_s = \hbar\mathbf{q}/2m_3$ and m_3 is the mass of a ^3He atom. The main quantities measured in the NMR experiment are the magnetic susceptibility χ and the shift of the resonance frequency $\delta\omega$ from the Larmor value. The former is obtained by evaluating f_z . The latter needs evaluating f_d in the dynamic case (Leggett 1974). The results for homogeneous A and B phases are

$$\rho_{sA} = \frac{8m_3^2}{\hbar^2} K \Delta_A^2 [\gamma + 1 - (\gamma - 1)(\hat{\mathbf{I}} \cdot \hat{\mathbf{v}}_s)^2] \quad (22)$$

$$\rho_{sB} = \frac{8m_3^2}{\hbar^2} (\gamma + 2) K \Delta_B^2 \quad (23)$$

$$\chi_A = \chi_n \quad (\hat{\mathbf{d}} \perp \mathbf{H}) \quad (24)$$

$$\chi_B = \chi_n - 2g_z \Delta_B^2 \quad (25)$$

$$\delta\omega_A = \frac{2\tilde{\gamma}}{\chi_n H} g_d \Delta_A^2 [(\hat{\mathbf{I}} \cdot \hat{\mathbf{d}})^2 - (\hat{\mathbf{I}} \cdot \hat{\mathbf{H}})^2] \quad (\hat{\mathbf{d}} \perp \mathbf{H}) \quad (26)$$

$$\delta\omega_B = \frac{15\tilde{\gamma}}{2\chi_n H} g_d \Delta_B^2 |\hat{\mathbf{n}} \times \hat{\mathbf{H}}|^2 \quad (\theta = 104^\circ). \quad (27)$$

Here $\hat{\mathbf{v}}_s$ and $\hat{\mathbf{H}}$ denote the directions of the superfluid velocity and field, respectively. The susceptibility of the normal phase χ_n has to include the inert layer of ^3He atoms on the aerogel strands, which in fact is the dominant contribution at low temperatures (Sprague et al. 1995). The frequency shifts $\delta\omega$ are for small tipping angles of the magnetization from the equilibrium direction $\hat{\mathbf{H}}$, and the magnetic field H is assumed large in comparison to $\sqrt{g_d/g_z} \approx 0.2$ mT. The results for χ_A , $\delta\omega_A$, and $\delta\omega_B$ are limited to the conditions indicated in parenthesis after each equation.

The NMR experiments with ^3He (no ^4He mixed) see no deviation of the susceptibility from χ_n (Sprague et al. 1995, 1996). In the HSM model, we interpret this as evidence for the A phase. Therefore, the measured frequency shift is best compared with $\delta\omega_A$. In Fig. 3(a) we plot the suppression factor

$$S_{\chi_n \delta\omega_A} \equiv \frac{\chi_n \delta\omega(tT_c)}{\chi_{n0} \delta\omega_{A0}(tT_{c0})} = \frac{\Delta^2(tT_c)}{\Delta_0^2(tT_{c0})} \equiv S_{\Delta^2}. \quad (28)$$

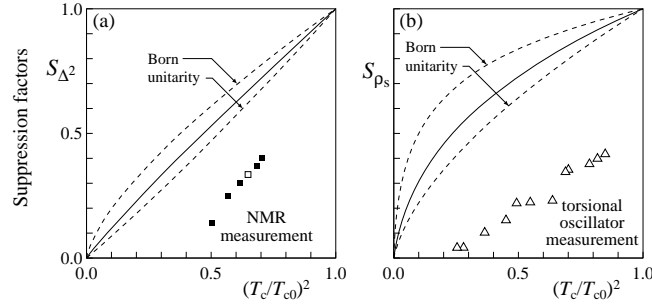


Fig. 3. The suppression factors for Δ^2 and ρ_s as a function of T_c reduction: $(T_c/T_{c0})^2$. The lines are theoretical results for the B phase when $t \rightarrow 1$ [see equations (28) and (29)]. The dashed lines denote Born and unitarity limits, and solid lines are for the intermediate case $\sin^2 \delta_0 = 0.5$. The data points are from Sprague et al. (1995, A type phase, \blacksquare), Sprague et al. (1996, B type phase, \blacksquare), and Porto and Parpia (1995, \triangle), all corresponding to $t \approx 0.9$.

Generally, the suppression factor is the ratio of a quantity in aerogel relative to the same quantity in the pure case. The latter is denoted by subindex 0. The ratio is taken at the same temperature t measured relative to the corresponding T_c . We consider here t in the range $0.9 \dots 1$ where the GL theory is expected to be valid. The middle equality (28) is based on equation (26). It is valid because g_d is a constant and the minimum-energy orientations of $\hat{\mathbf{d}}$ and $\hat{\mathbf{l}}$ are unchanged by scattering. (The latter is not necessarily satisfied in generalizations of the HSM, see Section 6.) Similarly we can define a suppression factor for ρ_s :

$$S_{\rho_s} \equiv \frac{\rho_s(tT_c)}{\rho_{s0}(tT_{c0})}. \quad (29)$$

The B phase ρ_{s0} is used as a reference in the experimental points of Fig. 3(b).

The theoretical suppression factors S_{Δ^2} and S_{ρ_s} are plotted in Fig. 3. In these the impure B phase is compared with bulk B phase. Very similar suppression factors are obtained when impure A phase is compared with bulk A phase: The solid lines are the same for Δ^2 and also for ρ_s (22) averaged over all orientations of the A phase [corresponding to $(\hat{\mathbf{l}} \cdot \hat{\mathbf{v}}_s)^2 \rightarrow \frac{1}{3}$]. The variation between Born and unitarity limits is slightly smaller in the A than in the B phase.

We see from Fig. 3 that HSM indeed gives a suppression of Δ^2 and ρ_s , but it is insufficient to explain quantitatively the measured suppression.

5 Inhomogeneous scattering models

The disagreement between the experiments and the HSM is clear in Fig. 3. We have checked that this failure does not arise from limitation to the neighborhood of T_c or to the s -wave scattering approximation. Also magnetic scattering does not seem to give a solution to this problem. We also discuss in Section 6 that the problem cannot be explained away by random anisotropy of the aerogel. Therefore it seems inevitable to sacrifice to basic assumption of the HSM: the homogeneity of the scattering.

A simple model of inhomogeneous scattering is to consider ${}^3\text{He}$ between two diffusively scattering planes. The transition temperature for this “slab model” is calculated by Kjaldman et al. (1978), and the suppression factors are evaluated by Thuneberg et al. (1996). This gave promising results (see Fig. 2) but it is not a suitable model for aerogel because of its strong anisotropy. Recently an “isotropic inhomogeneous scattering model” (IISM) was studied (Thuneberg et al. 1997). This is consistent with the observed isotropy of aerogel, and it gives rather good fits to both T_c and S_{Δ^2} . Because only preliminary calculations on the IISM has been done, we leave its discussion to another occasion. What is of importance here that part of the HSM seems to remain valid: Although the gap amplitude Δ^2 is badly overestimated in the HSM, the equations (22)-(27) for ρ_s , χ , and $\delta\omega$ may still constitute a reasonable approximation. This will be used in the following section. Similar arguments may be applied to the HSM calculations by Baramidze et al. (1996).

6 Anisotropic HSM

In this section we consider how to generalize the isotropic HSM (Section 4) to anisotropic scattering. The anisotropy will affect all the terms in the GL functional, but the most important effect comes from the modification of the second order bulk term (3). The anisotropy requires the replacement

$$\alpha A_{\mu i}^* A_{\mu i} \rightarrow \alpha_{ij} A_{\mu i}^* A_{\mu j} . \quad (30)$$

So the scalar α is replaced by a tensor $\underline{\alpha}$. Solving the quasiclassical equations in this case gives

$$\underline{\alpha} = \frac{N(0)}{3} \left\{ \ln \frac{T}{T_{c0}} + \sum_{m=1}^{\infty} \left[\frac{1}{m - \frac{1}{2}} - \left(m - \frac{1}{2} + \frac{\hbar v_f n}{4\pi T} \underline{\alpha}_{\text{tr}} \right)^{-1} \right] \right\} . \quad (31)$$

Unit matrices multiplying $m - \frac{1}{2}$, for example, are not shown explicitly. The transport cross-section tensor is defined by the double angular average

$$\underline{\alpha}_{\text{tr}} = \langle \hat{\mathbf{k}} \left[\sigma(\hat{\mathbf{k}})\hat{\mathbf{k}} - 4\pi \left\langle \frac{d\sigma}{d\Omega}(\hat{\mathbf{k}}, \hat{\mathbf{k}}') \hat{\mathbf{k}}' \right\rangle_{\hat{\mathbf{k}}'} \right] \rangle_{\hat{\mathbf{k}}} , \quad (32)$$

where $d\sigma/d\Omega$ is the differential scattering cross section and the total cross section $\sigma(\hat{\mathbf{k}}) = 4\pi \langle (d\sigma/d\Omega)(\hat{\mathbf{k}}, \hat{\mathbf{k}}') \rangle_{\hat{\mathbf{k}}'}$. [In equation (31) we have assumed that both $\hat{\mathbf{k}}$ and $\hat{\mathbf{k}}'$ dependencies of $(d\sigma/d\Omega)(\hat{\mathbf{k}}, \hat{\mathbf{k}}')$ can be represented by s and p -wave spherical harmonic functions.] For estimation of the anisotropy in aerogel we consider a long rod, which scatters diffusely (randomly) the particles hitting it. This gives $n\sigma_{\text{tr}} = \ell^{-1}(\frac{9}{8} - \frac{3}{8}\hat{\mathbf{a}}\hat{\mathbf{a}})$, where $\hat{\mathbf{a}}$ is the direction of the rod and ℓ denotes the average (transport) mean free path. Assuming the anisotropy is small, the leading effect of the anisotropy can be represented by

$$f_{\mathbf{a}} = -\alpha_1 \hat{a}_i A_{\mu i}^* A_{\mu j} \hat{a}_j, \quad (33)$$

where

$$\alpha_1 = \frac{N(0)\hbar v_{\text{f}}}{32\pi T_c \ell} \sum_{m=1}^{\infty} (m - \frac{1}{2} + x_c)^{-2}. \quad (34)$$

It is crucial that the anisotropy direction $\hat{\mathbf{a}}$ is not a constant. We expect that the orientational correlation decays in a length $L_{\mathbf{a}} \sim 20$ nm, which is on the order of the average distance between strands.

The anisotropy (33) shifts the transition temperature. It also changes the relative stability of different phases. Instead of discussing these, we will here concentrate on how the anisotropy can crucially modify the NMR properties. Some of the ideas below are suggested by Volovik (1996).

Quite generally, we can write the following hydrodynamic free energy for the A phase

$$\begin{aligned} f_{\text{A}} = & -\frac{1}{2}\lambda_{\text{d}}(\hat{\mathbf{d}} \cdot \hat{\mathbf{l}})^2 + \frac{1}{2}\lambda_{\text{z}}(\hat{\mathbf{d}} \cdot \mathbf{H})^2 + \frac{1}{2}\lambda_{\mathbf{a}}(\hat{\mathbf{a}} \cdot \hat{\mathbf{l}})^2 + \frac{1}{2}\rho_{\perp}\mathbf{v}_{\text{s}}^2 + \frac{1}{2}(\rho_{\parallel} - \rho_{\perp})(\hat{\mathbf{l}} \cdot \mathbf{v}_{\text{s}})^2 \\ & + C\mathbf{v}_{\text{s}} \cdot \nabla \times \hat{\mathbf{l}} - C_0(\hat{\mathbf{l}} \cdot \mathbf{v}_{\text{s}})(\hat{\mathbf{l}} \cdot \nabla \times \hat{\mathbf{l}}) + \frac{1}{2}K_{\text{s}}(\nabla \cdot \hat{\mathbf{l}})^2 + \frac{1}{2}K_{\text{t}}(\hat{\mathbf{l}} \cdot \nabla \times \hat{\mathbf{l}})^2 \\ & + \frac{1}{2}K_{\text{b}}|\hat{\mathbf{l}} \times (\nabla \times \hat{\mathbf{l}})|^2 + \frac{1}{2}K_5|(\hat{\mathbf{l}} \cdot \nabla)\hat{\mathbf{d}}|^2 + \frac{1}{2}K_6[(\hat{\mathbf{l}} \times \nabla)_i \hat{\mathbf{d}}_j]^2. \end{aligned} \quad (35)$$

The first two terms are already familiar from equations (19) and (20). The third is the anisotropy term (33) with $\lambda_{\mathbf{a}} = 2\alpha_1\Delta_{\text{A}}^2$. The rest arises from the gradient energy (12) when the A-phase order parameter (6) is substituted into it (Cross 1975). All the coefficients are proportional to Δ_{A}^2 . Because this common factor drops out in relative comparisons of the terms, our estimations below are independent of Δ_{A}^2 .

The idea is that the random field $\hat{\mathbf{a}}$ tries to orient the $\hat{\mathbf{l}}$ vector. However, the gradient energy strongly limits the variation of $\hat{\mathbf{l}}$ on the scale $L_{\mathbf{a}}$. Instead, $\hat{\mathbf{l}}$ varies only on a ‘‘orbital’’ scale $L_{\text{o}} \gg L_{\mathbf{a}}$. In addition, the $\hat{\mathbf{d}}$ vector varies on a ‘‘spin’’ scale L_{s} , which also is large in comparison to ‘‘aerogel’’ scale $L_{\mathbf{a}}$. We estimate L_{o} and L_{s} using arguments presented by Imry and Ma (1975). The exact functional (35) is approximated by

$$\begin{aligned} f_{\text{A}} \approx & -\frac{\lambda_{\text{d}}}{6} - \frac{\eta\lambda_{\text{d}}}{3\eta + 2[(L_{\text{s}}/L_{\text{o}})^{3/4} - 1]^2} \\ & + \frac{\lambda_{\mathbf{a}}}{6} - \frac{\eta\lambda_{\mathbf{a}}}{2} \left(\frac{L_{\mathbf{a}}}{L_{\text{o}}}\right)^{3/2} + \frac{K_{\text{s}}}{2L_{\text{s}}^2} + \frac{K_{\text{o}}}{2L_{\text{o}}^2}. \end{aligned} \quad (36)$$

This is a functional of only two variables, L_s and L_o . The first two terms constitute an interpolation of the dipole-dipole energy between two limits. The minimum energy $-\frac{1}{2}\lambda_d$ is obtained in the limit $L_s = L_o$. In the opposite limit $L_s \gg L_o$, the dipole-dipole energy consists of a random average $-\frac{1}{6}\lambda_d$ plus a fluctuation $-\frac{1}{2}\eta\lambda_d(L_o/L_s)^{3/2}$ (Imry and Ma 1975). The origin of the factor $(L_o/L_s)^{3/2}$ is that in a box of volume L_s^3 there are $N = (L_o/L_s)^3$ uncorrelated regions of $\hat{\mathbf{l}}$, and therefore the total fluctuation they produce is proportional \sqrt{N} . Here $\eta = 2/3\sqrt{5}$ is the standard deviation of $(\hat{\mathbf{n}} \cdot \hat{\mathbf{z}})^2$ for a random unit vector $\hat{\mathbf{n}}$. The third and fourth terms in (36) approximate similarly the anisotropy energy $\frac{1}{2}\lambda_a(\hat{\mathbf{a}} \cdot \hat{\mathbf{l}})^2$, but there only the limiting form $L_o \gg L_a$ is needed. The last two terms are simplified gradient energies of $\hat{\mathbf{d}}$ and $\hat{\mathbf{l}}$. We assume $K_s \approx 12K\Delta_A^2$ and $K_o \approx 6K\Delta_A^2$, where a factor 3 arises from the dimensionality of the space.

The simplified energy functional can now be trivially minimized numerically, and also to a great extent analytically. We find two basically different solutions, which are described below. These solutions have equal energy if $L_a = 48$ nm, which is only slightly larger than the estimated distance between stands 20 nm. The numerical estimates use this and the pressure of 2.8 MPa.

In the “dipole locked” solution $\hat{\mathbf{d}}$ and $\hat{\mathbf{l}}$ follow closely each other, $\hat{\mathbf{d}}(\mathbf{r}) \approx \hat{\mathbf{l}}(\mathbf{r})$. We find rather long $L_s \approx L_o \approx 70 \mu\text{m}$. The NMR experiments are done in large magnetic field, so that $\hat{\mathbf{d}} \approx \hat{\mathbf{l}}$ is allowed to vary only in the plane perpendicular to \mathbf{H} . We see from equation (26) that the NMR frequency shift $\delta\omega_A$ is essentially unchanged from the HSM prediction. This state has lowest energy for $L_a < 48$ nm.

In the “dipole unlocked” solution $\hat{\mathbf{l}}$ varies on a much shorter scale than $\hat{\mathbf{d}}$, $L_o \ll L_s$. We find $L_o \approx 8 \mu\text{m}$ and $L_s \approx 3$ mm. Again the magnetic field limits $\hat{\mathbf{d}}$ to the plane perpendicular to \mathbf{H} . However, $\hat{\mathbf{l}}$ is free to vary in all directions. The NMR frequency shift is totally suppressed: it is reduced by factor 10^{-5} relative to the HSM. This is because $\langle(\hat{\mathbf{l}} \cdot \hat{\mathbf{d}})^2\rangle \approx \langle(\hat{\mathbf{l}} \cdot \hat{\mathbf{H}})^2\rangle \approx \frac{1}{3}$ in the expression for $\delta\omega_A$ (26). This state has lowest energy if $L_a > 48$ nm.

As discussed above, the experiments see that the NMR frequency shift is smaller than the HSM prediction. However, they still are on the same order of magnitude. This strongly supports the dipole-locked state because in the unlocked state the suppression would be much more severe. Moreover, because the suppression in the locked state is unchanged from HSM, we reach the conclusion (stated in Section 5) that random anisotropy cannot explain the difference between measurements and the HSM.

The presence of the dipole-locked state of ^3He in aerogel implies that the anisotropy of aerogel is very small: it is equivalent to rods whose directions are correlated over distance $L_a < 48$ nm. This invalidates the slab model, because the thickness D of the slab is larger than this (see Fig. 2).

Above we have considered the NMR properties only in the case that the “tipping angle” β between the field and the magnetization is small. When the angle is increased, the frequency shift $\delta\omega$ gradually diminishes. This is similar to bulk $^3\text{He-A}$, and it is well understood theoretically (Brinkman and Smith 1975, Fomin

1978). However, the frequency shift suddenly disappears at about $\beta = 40^\circ$, and remains zero for all larger angles (Sprague et al. 1995). As suggested by Volovik (1996), this striking observation can be associated with the locked \rightarrow unlocked transition discussed above. At the time of writing this, this is still under study, so we postpone the discussion to another occasion.

7 Conclusion

We have extensively studied the homogeneous scattering model in the Ginzburg-Landau approximation. Although it fails to produce the correct gap amplitude, it may successfully be applied in the hydrodynamic region. As an example we considered NMR in the A phase. In the future it could be used, e.g., for studying vortices of ^3He in aerogel.

Acknowledgments

I thank my collaborators M. Fogelström, S.K. Yip, J.A. Sauls, R. Hänninen, and T. Setälä for various contributions to this work. Fruitful discussions with W. Halperin, J. Hook, J. Parpia, J. Porto, D. Rainer, D. Sprague, G. Kharadze, and G. Volovik are acknowledged.

Appendix

In this appendix we briefly explain how the Ginzburg-Landau coefficients (α , β_i , etc.) are calculated in the quasiclassical theory. An intermediate quantity in the calculation is the quasiclassical 4×4 matrix Green's function $\hat{g}(\hat{\mathbf{k}}, \mathbf{r}, \epsilon_m)$. The arguments are the direction of the momentum $\hat{\mathbf{k}}$, the location \mathbf{r} , and the Matsubara frequencies $\epsilon_m = \pi k_B T(2m + 1)$. The Green's function is determined from the Eilenberger equations

$$[i\epsilon_m \hat{\tau}_3 - \hat{v} - \hat{\rho} - \hat{\Delta}, \hat{g}] + iv_F \hat{\mathbf{k}} \cdot \nabla_{\mathbf{r}} \hat{g} = 0 \quad (37)$$

$$\hat{g} \hat{g} = -\pi^2 . \quad (38)$$

Here $\hat{\tau}_i$ denote the Pauli matrices in Nambu space, and $[A, B] = AB - BA$. For more details the reader is referred to the review article by Serene and Rainer (1983). The self-consistency equations for the diagonal \hat{v} and off-diagonal $\hat{\Delta}$ self-energies are given in formulas (5.10) of Serene and Rainer (1983). The impurity self-energy $\hat{\rho}(\hat{\mathbf{k}}, \mathbf{r}, \epsilon_m)$ equals $n(\mathbf{r}) \hat{t}(\hat{\mathbf{k}}, \hat{\mathbf{k}}, \mathbf{r}, \epsilon_m)$, where $n(\mathbf{r})$ is the concentration of the scattering centers. The \hat{t} -matrix of a single scattering center is determined by

$$\hat{t}(\hat{\mathbf{k}}, \hat{\mathbf{k}}', \mathbf{r}, \epsilon_m) = \hat{v}(\hat{\mathbf{k}}, \hat{\mathbf{k}}') + N(0) \langle \hat{v}(\hat{\mathbf{k}}, \hat{\mathbf{k}}') \hat{g}(\hat{\mathbf{k}}'', \mathbf{r}, \epsilon_m) \hat{t}(\hat{\mathbf{k}}'', \hat{\mathbf{k}}', \mathbf{r}, \epsilon_m) \rangle_{\hat{\mathbf{k}}''} . \quad (39)$$

Also we need the free energy functional which is given by equation (5.11) of Serene and Rainer (1983).

The coefficients are calculated by solving Green's function perturbatively $\hat{g} = \hat{g}_0 + \hat{g}_1 + \hat{g}_2 + \dots$. Here \hat{g}_0 is the normal state Green's function, and the subindex denotes order in $\hat{\Delta}$. Then one collects terms of order 0, 1, 2, and 3 in the Eileberger, self-consistency and \hat{t} -matrix equations, and solves them in each order. Substitution to energy functional gives the results α (8) and β_i (10). For other coefficients it is sufficient to limit to first order in $\hat{\Delta}$, but one has to do additional expansions in gradients and in magnetic field. Substitution to energy functional gives K (15), γ (16) and g_z (17). The dipole coefficient (18) is obtained using the dipole-dipole Hamiltonian (Leggett 1974) in the general energy functional (5.6) of Serene and Rainer (1983).

References

- Abrikosov A.A., Gorkov L.P. (1961): Zh. Eksp. Teor. Fiz. **39**, 1781 [Sov. Phys. JETP **12**, 1243 (1961)]
- Baramidze G., Kharadze G., Vachnadze G. (1996): Pisma Zh. Eksp. Teor. Fiz. **63**, 95 [JETP Lett. **63**, 107]
- Brinkman W.F., Smith H. (1975): Phys. Lett. A **51**, 449
- Buchholtz L.J., Rainer D. (1979): Z. Physik B **35**, 151
- Cross M.C. (1975): J. Low Temp. Phys. **21**, 525
- Fetter A.L. (1975): *Quantum Statistics and the Many-Body Problem*, eds. S.B. Trickey, W.P. Kirk and J.W. Dufty (Plenum, New York), 127
- Fomin I.A. (1978): J. Low Temp. Phys. **31**, 509
- Fricke J. (1988): Sci. Am. **258**, No. 5, 68
- Gorkov L.P. (1959): Zh. Eksp. Teor. Fiz. **37**, 1407 [Sov. Phys. JETP **37**, 998 (1960)]
- Imry Y., Ma S. (1975): Phys. Rev. Lett. **35**, 1399
- Kim S.B., Ma J., Chan M.H.W. (1993): Phys. Rev. Lett. **71**, 2268
- Kjälldman L.H., Kurkijärvi J., Rainer D. (1978): J. Low Temp. Phys. **33**, 577
- Larkin A.I. (1965): JETP Lett. **2**, 130
- Leggett A.J. (1974): Ann. Phys. **85**, 11
- Leggett A.J. (1975): Rev. Mod. Phys. **47**, 331
- Matsumoto K., Porto J.V., Pollack L., Smith E.N., Ho T.L., Parpia J.M. (1997): Phys. Rev. Lett. **79**, 253
- Mermin N.D., Stare C. (1973): Phys. Rev. Lett. **30**, 1135
- Porto J.V., Parpia J.M. (1995): Phys. Rev. Lett. **74**, 4667
- Sauls J.A., Serene J.W. (1981): Phys. Rev. B **24**, 183
- Serene J.W., Rainer D. (1983): Phys. Rep. **101**, 221
- Sprague D.T., Haard T.M., Kycia J.B., Rand M.R., Lee Y., Hamot P.J., Halperin W.P. (1995): Phys. Rev. Lett. **75**, 661
- Sprague D.T., Haard T.M., Kycia J.B., Rand M.R., Lee Y., Hamot P.J., Halperin W.P. (1996): Phys. Rev. Lett. **77**, 4568
- Tholen S.M., Parpia J.M. (1992): Phys. Rev. Lett. **68**, 2810
- Thuneberg E.V. (1987): Phys. Rev. B **36**, 3583
- Thuneberg E.V., Kurkijärvi J., Rainer D. (1981): J. Phys. C **14**, 5615
- Thuneberg E.V., Fogelström M., Yip S.K., Sauls J.A. (1996): Czechoslovak J. Phys. **46**, 113

Thuneberg E.V., Fogelström M., Yip S.K., Sauls J.A. (1997): <http://xxx.lanl.gov/abs/cond-mat/9601148>

Vollhardt D., Wölfle P. (1990): *The superfluid phases of helium 3* (Francis&Taylor, London)

Volovik G.E. (1996): Pis'ma Zh. Eksp. Teor. Fiz. **63**, 281